Adsorption 8: 59–70, 2002

CVD-Titania on Mesoporous Silica Gels

V.M. GUN'KO,* A.G. DYACHENKO AND M.V. BORYSENKO
Institute of Surface Chemistry, 17 General Naumov Street, 03164 Kiev, Ukraine
vlad-gun@carrier.kiev.ua

J. SKUBISZEWSKA-ZIĘBA AND R. LEBODA
Department of Chemical Physics, Maria Curie-Sklodowska University, 20031 Lublin, Poland

Abstract. Different amounts of CVD-titania (C_{TiO_2} from 2.3 to 19.2 wt%) with amorphous and crystalline (anatase) phases were synthesized on silica gels (Kieselgel 40, 60, and 100) and characterized by means of XRD, IR, DTG, and adsorption methods. The amounts of titania depend strongly on the pore size distribution of the support, as the narrower the pores, the lower the deposit concentration due to diminution of the accessibility of narrower pores and deceleration of titania grafting in them. A portion of CVD-titania filling matrix pores is rather amorphous than that forming on the outer (external) surfaces of silica gel grains, as anatase crystallites have the average size of 70 nm for KG 40/TiO_2 (C_{TiO_2} = 6.5 wt% including 26% of anatase and 74% of amorphous titania), 21 nm (KG 60/TiO_2 at C_{TiO_2} = 11 wt%, 16% anatase) and 16 nm (KG 100/TiO_2 at C_{TiO_2} = 19.2 wt%, 29% anatase), which are larger than the average pore size of the silica gels. The crystallite size decreases with increasing average pore diameter.

Keywords: CVD-titania/silica gel, adsorption, XRD, IR, pore size distribution, amorphous titania, anatase

1. Introduction

Titania/silica (TS) materials (gels, sieves, aerogels, thin films, fumed powder) are used as catalysts, adsorbents, pigments, etc., whose characteristics depend on synthesis method (chemical vapor deposition (CVD), sol-gel, precipitation, high-temperature hydrolysis, etc.), matrix type, conditions of pre-treatment, component concentrations and their distribution in the volume and at the surface, and phase composition. TSs studied previously (Castillo et al., 1994; Battiston et al., 1994; Vansant et al., 1995; Crocker et al., 1996; Hanprasopwattana et al., 1996; Leboda et al., 1999, 2000; Gun'ko et al., 1997–2000) were synthesized on different silicas by one or several reaction cycles under various conditions of liquid- or gas-phase reactions to obtain titania of different morphology, concentration (C_{TiO_2}) and phase (amorphous + crystalline) composition. The deposition method influences strongly the morphology and dispersion of the coated oxide; e.g., impregnation provides the best external superficial dispersion of titania allowing the formation of small crystallites at the surfaces, but the grafting method gives the best internal TiO_2 dispersion with formation of large crystallites at the external surface of silica (Castillo et al., 1994). However, the impact of the pore size distribution (PSD) of different silica matrices on the characteristics of titania grafted under the same and mild conditions was explored inadequately. Therefore, the aim of this work was to study the influence of the texture of silica gels with different PSD on the structural and adsorptive properties of CVD-titania (synthesized with different numbers of reaction cycles under the same and mild conditions) and TS adsorbent as a whole.

*To whom correspondence should be addressed.

2. Experimental Section

2.1. Materials

Titania was deposited on the surfaces of such mesoporous silica gels as Kieselgel 40, KG 40, (grain fraction 0.2–0.5 mm), Kieselgel 60, KG 60, (0.1–0.2 mm), and Kieselgel 100, KG 100, (0.1–0.2 mm) (Merck) using $TiCl_4$ (Aldrich) additionally purified by distillation and water vapor as reactants. Structural features of similar silica gels pristine and modified are described in detail elsewhere (Vansant et al., 1995; Legrand, 1998; Kiselev and Lygin, 1972). A silica sample (1–4 g) placed into a quartz flow-type reactor (rotated in order to make dehydration, modification and hydrolysis more uniformly) was heated (for dehydration) in the argon stream (20 $cm^3 \cdot min^{-1}$) at 523 K for 2 h. Then argon saturated with $TiCl_4$ was let in the reactor to modify the silica surfaces at 523 K for 1 h. Thereupon the argon flow was used to remove the reaction products and the residual modifier at the same temperature for 30 min. Next water-vapor treatment of $TiCl_x$ groups bonded to the surfaces was carried out at 523 K for 1 h. The water excess and the volatile products were removed by the argon flow under the same conditions. The dehydration-modification-hydrolysis

$$(\equiv\mathrm{Si{-}OH})_n \ldots (\mathrm{OH_2})_m \ldots (\mathrm{O(H)Si}\equiv)_1 \rightarrow (\equiv\mathrm{Si{-}OH})_{n+1} + m(\mathrm{H_2O})\uparrow \quad (1)$$

$$n(\equiv\mathrm{Si{-}OH}) + \mathrm{TiCl_4} \rightarrow (\equiv\mathrm{Si{-}O{-}})\mathrm{TiCl}_{4-n} + n(\mathrm{HCl})\uparrow \quad (2)$$

$$(\equiv\mathrm{Si{-}O{-}})_n\mathrm{TiCl}_{4-n} + (4-n)\,\mathrm{H_2O} \rightarrow (\equiv\mathrm{Si{-}O{-}})_n\mathrm{Ti(OH)}_{4-n} + (4-n)\mathrm{HCl}\uparrow \quad (3)$$

$$n(\equiv\mathrm{Ti{-}OH}) + \mathrm{TiCl_4} \rightarrow (\equiv\mathrm{Ti{-}O{-}})\mathrm{TiCl}_{4-n} + n(\mathrm{HCl})\uparrow \quad (4)$$

$$(\equiv\mathrm{Ti{-}O{-}})_n\mathrm{TiCl}_{4-n} + (4-n)\,\mathrm{H_2O} \rightarrow (\equiv\mathrm{Ti{-}O{-}})_n\mathrm{Ti(OH)}_{4-n} + (4-n)\mathrm{HCl}\uparrow \quad (5)$$

was reiterated up to four times to increase a titania loading, which (as well as the increment in C_{TiO_2}) strongly depends on PSD (Table 1). Reactions (2) and (4) correspond to the electrophilic substitution mechanism (S_Ei), and Eqs. (3) and (5) are related to the nucleophilic substitution mechanism (S_Ni). A limiting stage of these reactions corresponds to H^+ transferring in a cyclic transition state (TS). Under the S_Ei mechanism, H^+ transfers from the surface hydroxyls to Cl in a reactant molecule, but for S_Ni, the H^+ transferring direction is opposite—from water molecule to Cl in a surface group and this reaction also occurs through the cyclic TS. The probability of reactions between $TiCl_4$ and bridges ≡Si—O—Si≡, ≡Si—O—Ti≡, and ≡Ti—O—Ti≡ under soft conditions ($T_r < 523$ K) is significantly lower than that for reactions (2) or (4), as electron-donor properties of the oxygen atoms in these bridges are weaker than those for the OH groups. At higher temperatures ($T_r > 700$ K), the probability of the $TiCl_4$ interaction with the mentioned bridges increases, that leads to titania consolidation and an increase in the area of contacts between titania and silica support and a rutile portion in titania deposits grows (Vansant et al., 1995; Crocker et al., 1996; Leboda et al., 1999, 2000; Gun'ko et al., 1997–2000).

Table 1. Concentrations of anatase and amorphous titania in CVD-TiO_2/silica gel.

	TiO_2 concentration (wt%)		
Sample	Total	Anatase	Amorphous
KG 40-1	2.3	0	2.3
KG 40-2	4.7	1.3	3.4
KG 40-3	5.7	1.5	4.2
KG 40-4	6.5	1.7	4.8
KG 60-1	2.5	0	2.5
KG 60-2	4.5	0.8	3.7
KG 60-3	8.5	1.6	6.9
KG 60-4	11.0	1.8	9.2
KG 100-1	2.5	0.5	2.0
KG 100-2	7.2	2.1	5.1
KG 100-3	10.7	3.6	7.1
KG 100-4	19.2	5.6	13.6

Hydrolysis of ≡Si—O—Ti≡ bonds (≡Si—O—Ti≡ + H_2O → ≡Si—O—Ti≡ ← OH_2 → ≡Si—OH + HO—Ti≡) occurs through the S_Ni mechanism with formation a donor-acceptor bond Ti ← OH_2 in the intermediate. Since T_r (523 K) was not high, the probability of other mechanisms, e.g. related to radical reactions, was low. On heating of samples, segregation of titania can occur with formation of relatively large particles; however, the size of these particles formed in pores is restricted by the pore width, but the particles formed on the outer (external) surfaces of the support can be significantly larger. Notice that the coordination number of Ti atoms on the surfaces can be between 4 (on silica in groups $(\equiv\mathrm{Si{-}O{-}})_n\mathrm{Ti(OH)}_{4-n}$) and 6 on titania particles, and

there are terminal ≡SiOH and ≡TiOH and bridging ≡TiO(H)Ti≡ groups, whose structure and properties can influence the reactions and the product composition and morphology. Therefore the dehydration temperature can impact subsequent CVD reactions, as possible reduction of the concentration of the ≡SiOH groups (as reactive sites) causes diminution of the number of titania growth centers. Elevating of the reaction temperature from 473–523 K (amorphous titania and antase can be formed) to $T_r = 873$ K causes appearance of the rutile phase (with denser particles than formed at lower T_r), whose concentration increases with T_r. Subsequent treatment of titania/silica at temperature higher than T_r has a weak influence on the ratio between the concentrations of anatase and rutile, since the silica matrix inhibits the change of phase (anatase → rutile) at the temperature higher than that of this process for individual titania (Vansant et al., 1995; Crocker et al., 1996; Leboda et al., 1999, 2000; Gun'ko et al., 1997–2000).

The CVD-TiO_2/silica gel samples have various titania loading ranged from 2.3 to 19.2 wt% (Table 1) labeled as KG $40-x$, KG $60-x$, and KG $100-x$, where x denotes a number of reaction cycles from 1 to 4 on CVD of TiO_2 onto the Kieselgel surfaces. The total titanium content in TS samples was determined analyzing Ti(IV) peroxy complexes in the acidic solution with a KFK-2MP (LOMO, St. Petersburg) spectrophotometer at 400 nm and re-computed in respect to C_{TiO_2} (Table 1). In order to be sure that all titanium was released from the TS samples, silica was removed by heating with hydrofluoric acid, and titania was diluted by boiling with concentrated sulphuric acid.

2.2. X-ray Powder Analysis

X-ray diffraction (XRD) patterns (Fig. 1) were recorded over the 5–60° (scanning step 0.1°) and 24–30° (0.01°) ranges with a DRON-3M (LOMO, St. Petersburg) diffractometer using Cu K_α ($\lambda = 0.15418$ nm) radiation and Ni filter. The average size of anatase crystallites was estimated according to the Scherrer equation.

2.3. Infrared Spectroscopy

The IR spectra were recorded by means of a Specord M80 (Karl Zeiss, Jena) spectrophotometer using low amounts of oxide samples, which were well stirred with nujol mull, then placed between KBr glasses.

2.4. Nitrogen Adsorption

The specific surface area (Table 2, S_{BET}) computed using standard BET equation (Gregg and Sing, 1982; Adamson and Gast, 1997), the pore volume V_p (estimated at $p/p_0 \approx 0.98$, where p and p_0 denote the equilibrium and saturation pressures of nitrogen, respectively, converting the volume of adsorbed nitrogen to the volume of liquid one), the average pore radius R_p (for a cylindrical pore model) and other pore parameters listed in Table 2 were determined from nitrogen adsorption-desorption at 77.4 K measured by using a Micromeritics ASAP 2010 adsorption analyzer. The α_S plots (Gregg and Sing, 1982; Adamson and Gast, 1997) were utilized to estimate the specific surface area of mesopores (S_α) (silica gel Si-1000 was used as a reference material (Jaroniec et al., 1999)). One can assume that the reference adsorption on Si-1000 is appropriate for the studied TS materials, as the concentrations of titania are not large (Table 1) and the silica surface is not covered by a continuous TiO_2 layer; besides, features of non-specific adsorption of nitrogen are determined mainly by pore shape.

The PSDs $f(R_p)$ were calculated using the overall isotherm equation based on the combination of the modified Kelvin equation and the statistical adsorbed film thickness (Nguyen and Do, 1999) applied to a model of cylindrical pores for silica gel

$$a = \int_{r_{\min}}^{r_k(p)} f(R_p)\, dR_p + \int_{r_k(p)}^{r_{\max}} \frac{w}{R_p} t(p, R_p) f(R_p)\, dR_p \tag{6}$$

where $r_{\min}$ and $r_{\max}$ are the minimal and maximal pore radii, respectively; $w = 2$ for cylindrical pores; $r_k(p)$ is determined with the modified Kelvin equation

$$r_k(p) = \frac{\sigma_s}{2} + t(p, R_p) + \frac{w\gamma v_m \cos\theta}{R_g T \ln(p_0/p)} \tag{7}$$

and $t(p, R_p)$ can be computed with the modified BET equation

$$t(p, R_p) = t_m \frac{cz}{(1-z)} \frac{[1 + (nb/2 - n/2)z^{n-1} - (nb+1)z^n + (nb/2 + n/2)z^{n+1}]}{[1 + (c-1)z + (cb/2 - c/2)z^n - (cb/2 + c/2)z^{n+1}]}$$

$t_m = a_m / S_{BET}$; $b = \exp(\Delta\varepsilon / R_g T)$; $\Delta\varepsilon$ is the excess of the evaporation heat due to the interference of the

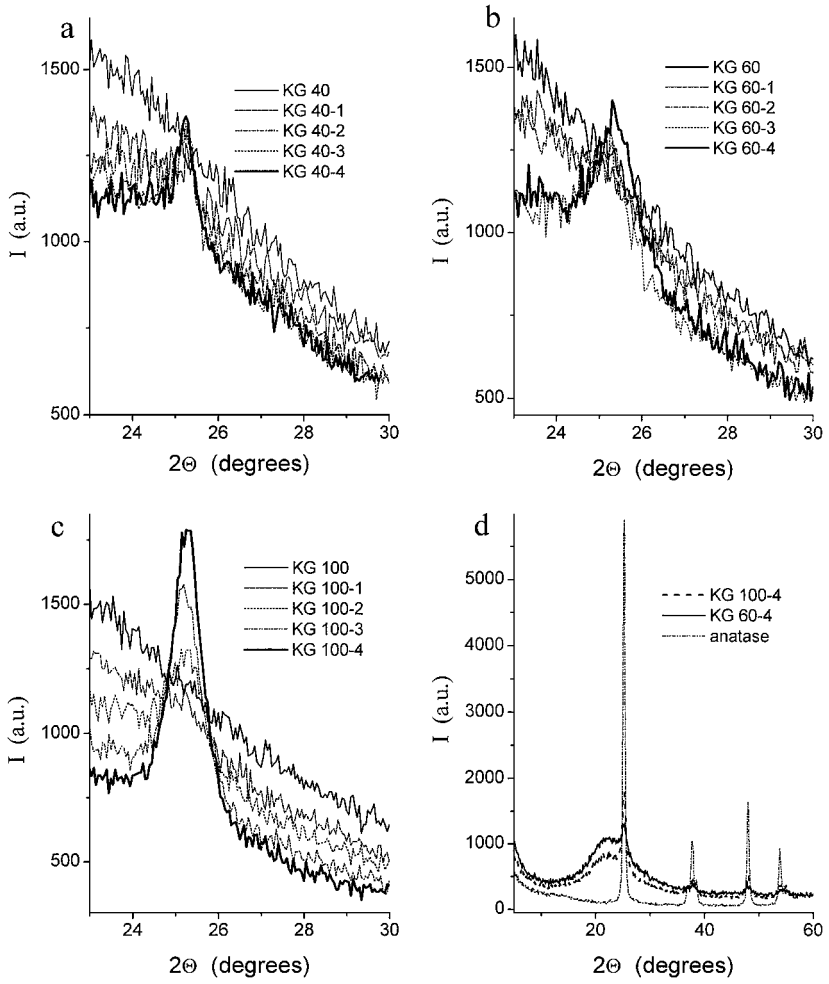

Figure 1. XRD patterns for (a) KG $40-x$, (b) KG $60-x$, (c) KG $100-x$ at $2\Theta = 23$–30°; (d) pure anatase; KG 60-4 and KG 100-4 at maximal titania loading.

layering on the opposite wall of pores (typically $\Delta\varepsilon$ is less than 3 kJ/mol for nitrogen molecules, $\Delta\varepsilon \approx$ 2.2 kJ/mol was used by Nguyen and Do, 1999); $t(p, R_p)$ is the statistical thickness of adsorbed layer; a_m is the BET monolayer capacity; $c = c_s \exp((Q_p - Q_s)/R_gT)$; c_s is the BET coefficient for adsorption on flat surface; Q_s and Q_p are the adsorption heat on flat surface and in pores, respectively; $z = p/p_0$; n is the number (non-integer) of statistical monolayers of adsorbate molecules and its maximal value for given R_p is equal to $(R_p - \sigma_S/2)/t_m$; and σ_s is the collision diameter of surface atoms. The desorption data were utilized to compute the $f(R_p)$ distribution with Eq. (6) and regularization procedure under non-negativity condition with a fixed regularization parameter $\alpha = 0.01$ (Provencher, 1982; Szombathely et al., 1992; Gun'ko and Do, 2001) within the scope of the cylindrical pore model for silica gels.

Calculation of the fractal dimension (Table 2, D_{AJ}) of the adsorbents was performed using adsorption isotherm equation (Avnir and Jaroniec, 1989) at $p/p_0 \leq 0.85$ with consideration for capillary condensation (nitrogen adsorption-desorption isotherms have marked hysteresis loops (Fig. 2)) in mesopores.

To characterize the adsorptive properties of titania/silica gels in comparison with pristine Kieselgels, the adsorption potential distributions $f(A) = -da/dA$ (where a denotes the adsorbed amount of nitrogen; $A = -\Delta G = R_gT \ln(p_0/p)$ is the differential molar work equal to the negative of the change of the Gibbs free energy; R_g is the gas constant) can be also utilized.

Table 2. Structural characteristics of silica gel and titania/silica gel samples.

Sample	S_{BET} (m^2/g)	V_p (cm^3/g)	S_α (m^2/g)	R_p (nm)	D_{AJ} $p/p_0 < 0.85$
KG 40	774	0.591	845	1.53	2.624
KG 40-1	677	0.515	743	1.52	2.640
KG 40-2	649	0.498	708	1.54	2.662
KG 40-3	641	0.492	699	1.54	2.664
KG 40-4	623	0.473	675	1.52	2.643
KG 60	461	0.807	497	3.50	2.421
KG 60-1	465	0.757	596	3.26	2.396
KG 60-2	450	0.765	478	3.40	2.419
KG 60-3	420	0.699	446	3.32	2.425
KG 60-4	427	0.701	455	3.29	2.431
KG 100	332	1.058	321	6.38	2.460
KG 100-1	336	1.049	338	6.23	2.461
KG 100-2	314	0.980	318	6.23	2.455
KG 100-3	299	0.912	301	6.10	2.460
KG 100-4	262	0.796	262	6.09	2.463

2.5. *Differential Thermogravimetry*

Differential thermal analysis and thermogravimetry were performed for oxide samples by using a Q-1500D (Paulik, Paulik & Erdey, MOM, Budapest) DTG apparatus. Oxide samples (415 ± 80 mg of KG or TS) exposed in saturated water vapor for 15 h were placed to a corundum crucible at room temperature and heated to 1280 K in air at a controlled heating rate 10 K/min. Since the time of entire saturation of mesoporous silica gels is approximately 70 h, exposition in the shorter time was applied to characterize the difference in water adsorption-desorption process depending on the texture of the adsorbents.

3. Results and Discussion

According to chemical analysis and XRD measurements, the total amounts of titania (amorphous + crystalline) (Fig. 3(a)) and the concentration of crystalline phase (anatase) (Fig. 3(b)) increase significantly with increasing pore size (Table 2, R_p) from KG 40 to KG 100, especially with increasing number of reaction cycles (Figs. 1 and 3, Tables 1 and 2), as formation of crystallites occurs preferably on the external surfaces, but smaller amorphous particles can form both in pores and on the external surfaces (Castillo et al., 1994; Vansant et al., 1995; Crocker et al., 1996). The titania portions representing anatase crystallites deposited on KG 40 and KG 60 under the same conditions (the same number of reaction cycles) are close (Fig. 3(b)). At the same time, the average size of these crystallites is significantly smaller for KG 60 (one can assume that a portion of these crystallites forming in pores of KG 60 is larger than that for KG 40). However, the total amounts of titania grafted on KG 60 are greater (Fig. 3(a), Table 1), as its pore volume V_p and average pore radius R_p are larger than those for KG 40 (Table 2) and amorphous titania with tiny particles can form in pores of the matrices. The relative concentration of amorphous titania $\gamma = C_{\text{amorphous } TiO_2}/C_{TiO_2}$ is maximal for TiO_2/KG 60 and minimal for TiO_2/KG 100 for all the numbers of the reaction cycles (Fig. 3(c)). Notice that the γ value changes slightly for each KG matrix at $x = 2$–4 and it is maximal at minimal concentration of CVD-titania after the first reaction cycle ($x = 1$). This effect can be caused by preferable deposition of titania (on subsequent reaction cycles at $x = i + 1$) rather on to titania formed previously (at $x = i$) than onto the accessible silica surfaces due to difference in the reactivity of hydroxyls on silica and titania surfaces, the instability of Si—O—Ti bridges on hydrolysis, and the differences in the spatial structure of the titania and silica lattices. These circumstances also explain why large anatase crystallites (detected by using the XRD method) can form on the external surfaces of silica grains.

It is well known that grafted titania does not cover the total surface of the silica supports by the continuous layer even at large TiO_2 amounts, as titania can represent not only tiny amorphous grains in support pores but also relatively large individual particles on the outer (external) silica surfaces (Gun'ko et al., 1997–1999; Leboda et al., 1999, 2000; Crocker et al., 1996). Evaluation of the mean size of anatase crystallites (at the maximal loading of titania) using the Scherrer equation gives 70 nm for KG 40-4, 21 nm (KG 60-4), and 16 nm (KG 100-4). These average sizes are larger than the average pore sizes of the silica supports (Table 2, $2 \times R_p$). This difference decreases with increasing average R_p for different KG due to formation of a portion of titania crystallites in silica gel pores of larger sizes. Formation of the largest titania particles (possessing low specific surface area per se) on the outer surface of KG 40 is due to both preferable formation of subsequent portions of titania on already formed TiO_2 nuclei and a low accessibility of the surfaces of narrow and partially blocked pores of TiO_2/KG 40 for $TiCl_4$

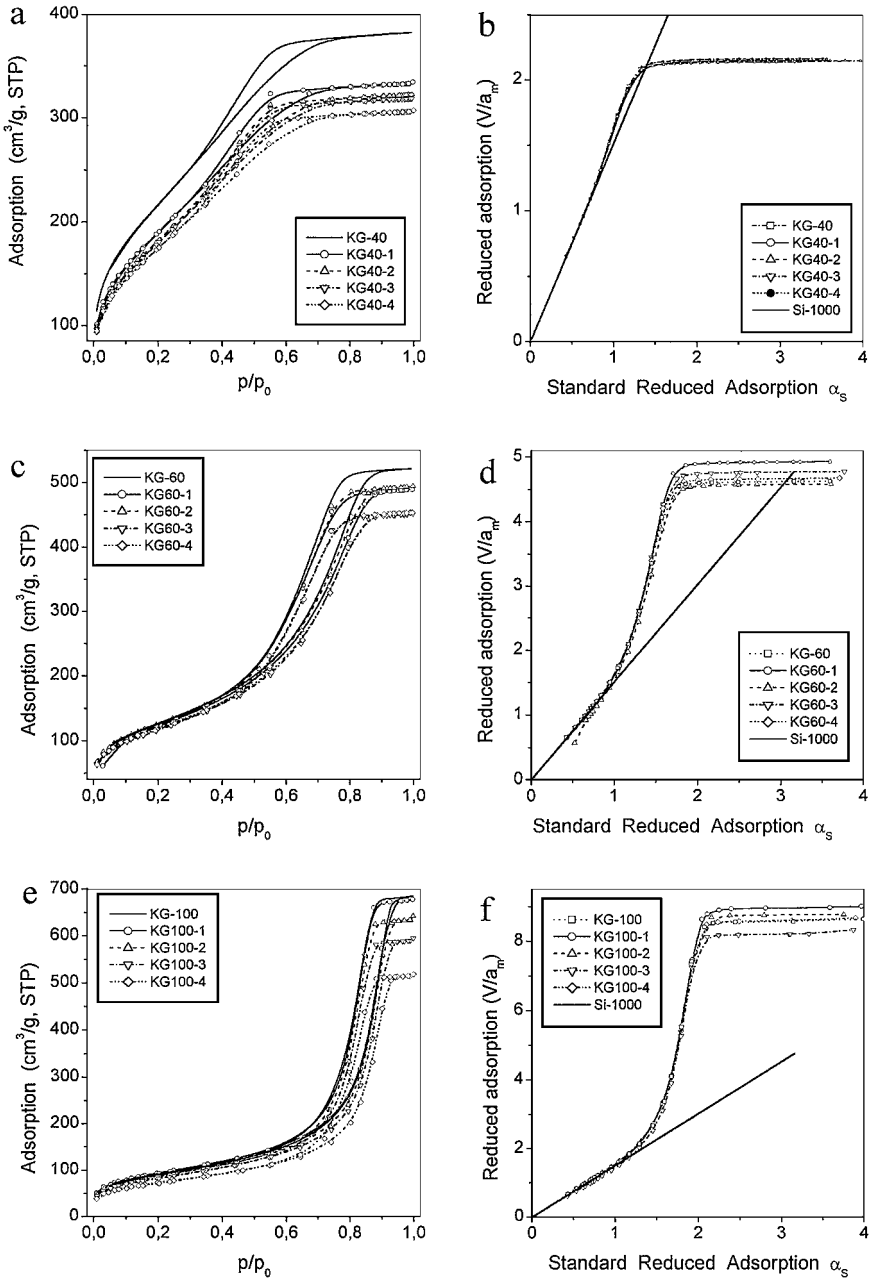

Figure 2. Nitrogen adsorption-desorption isotherms for (a) KG $40-x$; (c) KG $60-x$; (e) KG $100-x$ and the α_S plots reduced by dividing by a_m for (b) KG $40-x$; (d) KG $60-x$; (f) KG $100-x$.

molecules. Besides, one can assume that narrow pores in KG 40 are poorly accessible for titania deposition already after the first CVD cycle. The titania amounts grafted on the first reaction cycle are nearly the same for all silica gels (Table 1) but it inhibits subsequent formation of titania differently depending on the PSDs of modified silica gels, i.e., the accessibility of pores that causes changes in the increment of C_{TiO_2} with the reaction cycle number depending also on the PSD.

The IR spectra (Fig. 4) show that ≡Si—O—Ti≡ bonds in TS are practically absent, as the spectra over the 960–940 cm^{-1} range (characteristic for asymmetrical bridges ≡Si—O—Ti≡, i.e. $\nu_{SiO(Ti)}$, (Gun'ko et al., 1997–1999)) do not change after titania grafting. This result

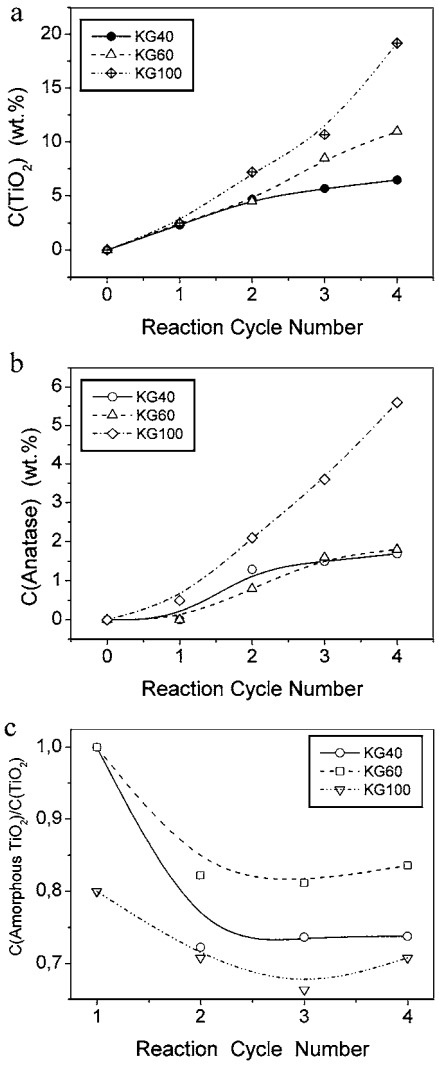

Figure 3. Relationships between the reaction cycle number and (a) total titania amounts; (b) anatase concentration; (d) relative contribution of amorphous titania.

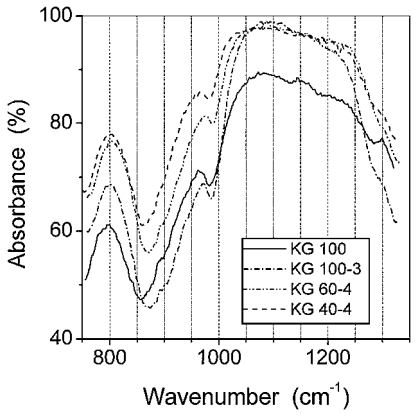

Figure 4. IR spectra of pristine KG 100 and CVD-titania/silica gels at the maximal loading of TiO_2.

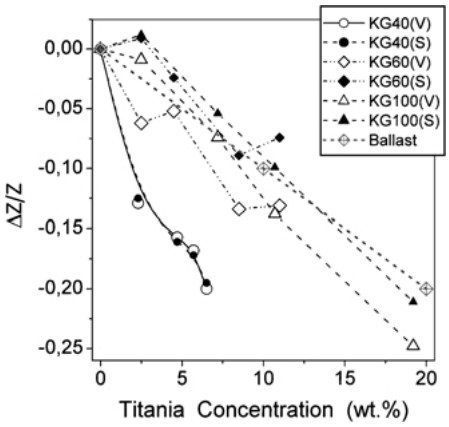

Figure 5. Relative changes in the pore volume ($Z = V_p$) and the specific surface area ($Z = S_{BET}$) as functions of the total titania amounts.

expected for silica/CVD-titania (synthesized using hydrolysis as one of the process stages) independent on silica kind (e.g., silica gel, fumed silica) is linked to hydrolysis not only of the residual Ti—Cl bonds but also of the unstable ≡Si—O—Ti≡ bonds and segregation of titania into individual particles during the synthesis (especially on the hydrolysis-heating stage).

The α_S plots (Fig. 2) show that relative changes in reduced adsorption are minimal for KG $40 - x$, but for KG $60 - x$ and KG $100 - x$, they are larger, similar and related mainly to the position of plateau adsorption (i.e. total pore volume V_p). Changes in V_p are very close to those for S_{BET} for KG $40 - x$ at any x, but those differ for other TS samples and this difference is larger for KG $60 - x$ (Fig. 5) due to features of the titania deposit morphology mentioned above (relatively large portion of small amorphous titania particles with a marked own specific surface area form in pores that results in the difference in $\Delta V_p/V_p$ and $\Delta S_{BET}/S_{BET}$ as functions of C_{TiO_2}). On the basis of these graphs, XRD data and previous investigations (Gun'ko et al., 1997–1999; Leboda et al., 1999, 2000; Crocker et al., 1996), one can assume that titania particles plug the silica gel pores maximum for KG $40 - x$ and minimum for KG $100 - x$. For KG 100, the titania deposit effect is close to that for pure ballast, which does not contribute to (i) the pore volume, (ii) the specific surface area, and (iii) blocking of matrix pores. However, the decline of the $\Delta V_p/V_p(C_{TiO_2})$ and $\Delta S_{BET}/S_{BET}(C_{TiO_2})$ plots for KG $100 - x$ is slightly greater than that for the ballast

line (Fig. 5); i.e., for the studied silica even with the largest pores, blocking of their portion by titania deposits occurs too. Note that for KG 60-1 and KG 100-1 (i.e. at low C_{TiO_2}), $\Delta V_p/V_p < 0$ but $\Delta S_{BET}/S_{BET} > 0$ due to formation of small titania particles (mainly amorphous even for KG 100, Table 1) possessing the specific surface area larger than that of the support. At the same time, $\Delta S_{BET}/S_{BET}$ and $\Delta V_p/V_p$ are significantly below zero for KG 40-1 and the graphs for KG-40 $-$ x lie markedly lower than that for the pure ballast (Fig. 5) due to blocking of a marked portion of pores by titania deposits. Notice that 6.5 wt% TiO_2 in KG-40-4 reduces the pore volume by 20% and 19.2 wt% TiO_2 in KG-100-4 reduces V_p by 25%, but one should consider the difference in the specific density of silica and titania, i.e., the last effect in respect to the volume unit is yet lower for KG-100-4. Thus, in all the cases, crystalline CVD-titania particles mainly form on the outer surfaces of silica grains or in maximum large pores or at the entry into mesopore (external surfaces) that results in blocking of a portion of pores depending on the type of silica gel. However, amorphous titania consisting of smaller particles can form in pores of silica gel especially in the case of KG 100 and KG 60. Thus, the narrower the pores, the larger the crystalline titania particles and the greater the pore blocking by these particles with decreasing total amount of titania deposits.

According to the XRD data and textural characteristics of the supports, the morphology of titania particles depends on the PSD of silica. This effect is confirmed by nonlinear dependences of $\Delta Z/Z = \Delta S_{BET}/S_{BET}$ or $\Delta V_p/V_p$ on C_{TiO_2} (Fig. 5) as well as fractal dimension D_{AJ} versus C_{TiO_2} (Fig. 6). For KG 40 $-$ x and KG

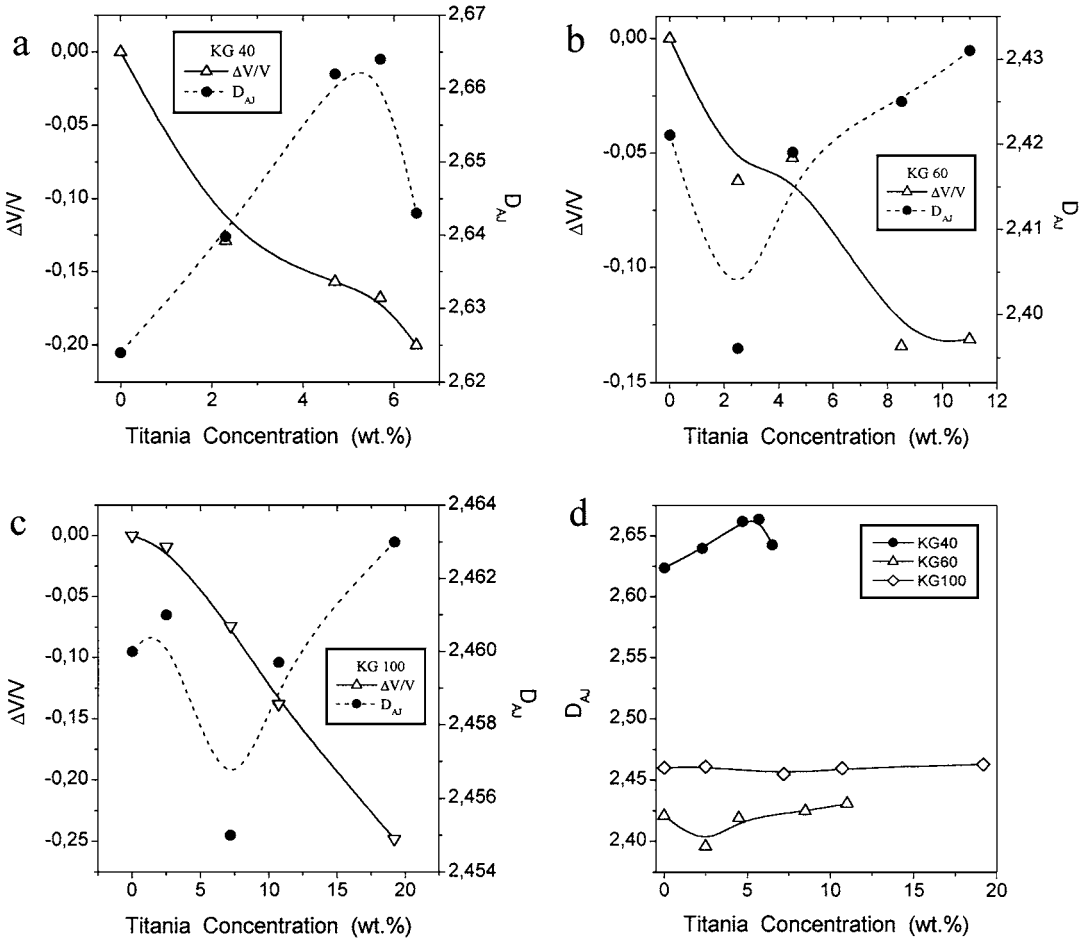

Figure 6. Relationships between total titania amounts and (a–d) fractal dimension D_{AJ} and changes in (a–c) the pore volume $\Delta V_p/V_p$ for (a) KG 40 $-$ x; (b) KG 60 $-$ x; (c) KG 100 $-$ x.

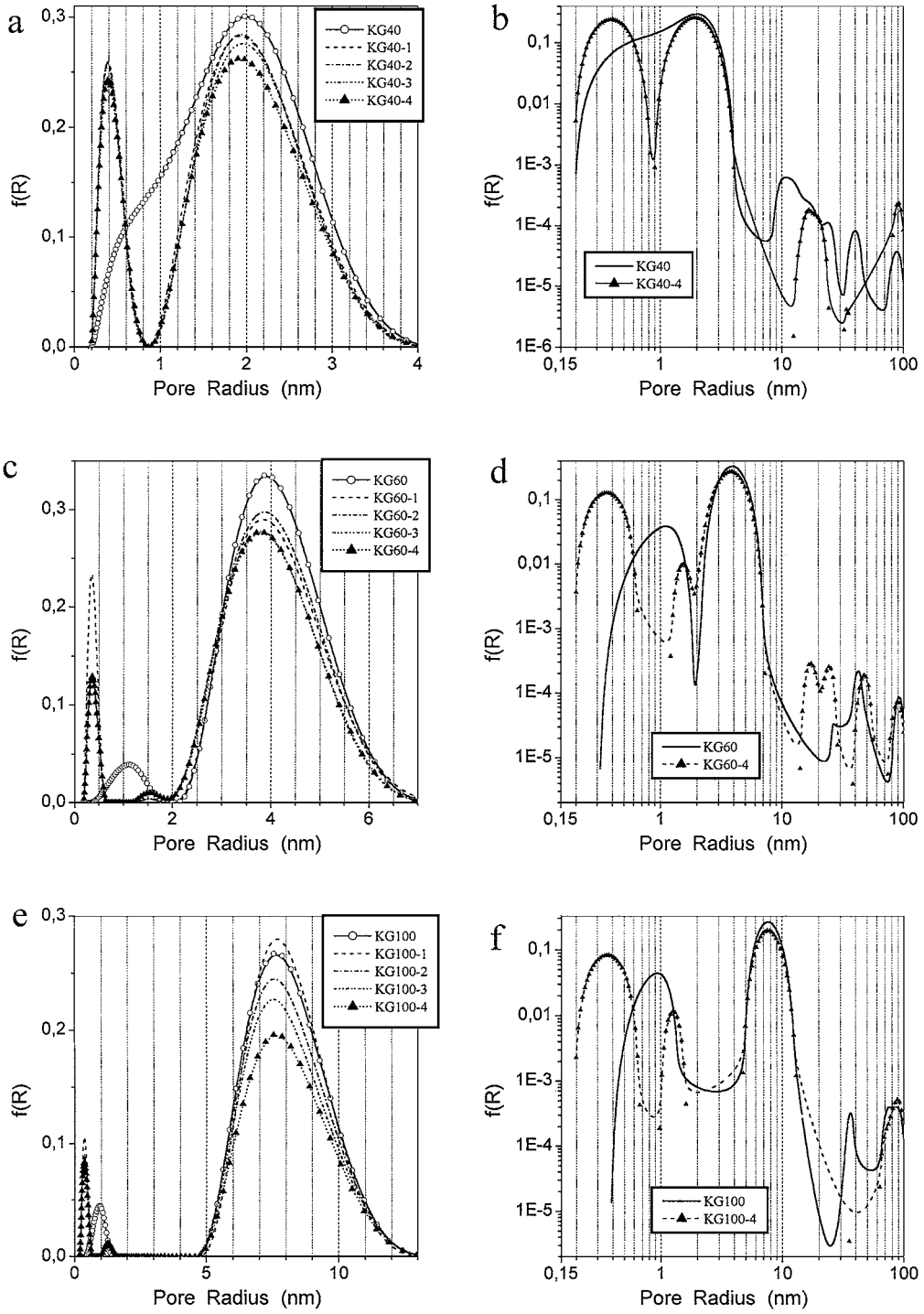

Figure 7. Pore size distributions in respect to dV_p/dR_p calculated with the regularization procedure at fixed regularization parameter $\alpha = 0.01$ for (a, b) KG 40 $-$ x; (c, d) KG 60 $-$ x; and (e, f) KG 100 $-$ x.

$60-x$ (or KG $100-x$), the $D_{AJ}(C_{TiO_2})$ graphs differ strongly. Note that the fractal dimension D_{AJ} can be connected to both the surface fractality (roughness of TS surfaces) and pore fractality of the silica gel supports partially filled by amorphous titania, and the fractality is minimal for KG $60-x$ (Table 2) including a maximal portion of amorphous titania (Fig. 3(c)) with small particles. Consequently, these structural features of TS samples can be caused by both titania particle structure (Figs. 1, 3 and 5) and PSDs (Fig. 7). From log-log graphs (Fig. 7), one can see that narrower micropores at $R_p < 1$ nm appear due to grafted titania (which can be caused partially by the gaps between titania particles and silica surface) independent of the silica support kind. Besides, large mesopores at $R_p > 10$ nm (possessing, however, a low total volume) are filled by titania deposits, as according to the XRD, average crystallite sizes >10 nm (amorphous titania particles can be significantly smaller than 10 nm). A small displacement of the main mesopore $f(R_p)$ peaks for TS samples is due to partial filling of these pores by titania particles. However, this effect is weak, as (i) the amounts of grafted titania are relatively low; (ii) specific density of titania is greater than that of silica; (iii) a portion of titania is connected with larger TiO_2 particles formed on the outer (external) surfaces of silica gel grains. Since, if all the titania particles form in silica gel pores that the main $f(R_p)$ peak displacement toward smaller R_p (due to narrowing of pores) would be proportional to C_{TiO_2}, however, this effect is very weak (Fig. 7). In the case of filling of smaller and larger pores in proportion to their volume one can expect nearly the same position of the main $f(R_p)$ peak; nevertheless pores narrower than those in the initial adsorbent should appear. A small diminution of average R_p observed for titania/KG 60 and KG 100 with C_{TiO_2} (Table 2) can be linked to filling of pores by amorphous titania and a portion of large pores (e.g., transport pores) by titania crystallites, as well as due to weighting of particles (as the specific density of titania is greater than that of silica) and reduction of the empty space (partially filled by titania) between silica gel grains.

The adsorption potential of TS samples decreases due to titania deposits (Fig. 8). A minimal difference in $f(A)$ for pristine and modified silica gels is observed for KG 60 and KG 60-4 with a maximal contribution of amorphous titania. A $f(A)$ maximum at $A < 1$ kJ/mol (corresponding to secondary (volume) filling of mesopores) shifts toward smaller A values with increasing pore size and this effect is practically independent of the

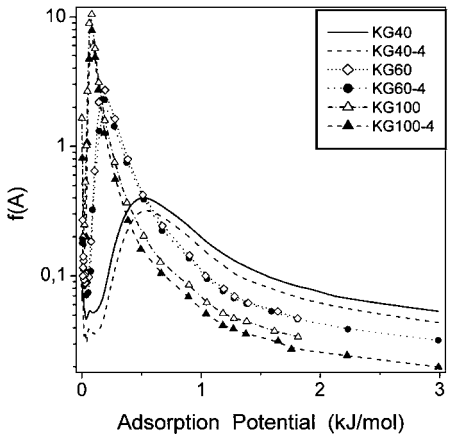

Figure 8. Adsorption potential distributions for pristine silica gels and TS at the maximal loading of titania.

nature of adsorbent surfaces, as only the first monolayer of nitrogen molecules is sensitive to the nature (silica or titania) of adsorption sites. For instance, the adsorption energy of N_2 interacting with terminal ≡SiOH and terminal ≡TiOH or bridging ≡TiO(H)Ti≡ groups equals to 8–9 kJ/mol and 11–25 kJ/mol, respectively, computed for oxide clusters with several polyhedrons using the DFT method with the B3LYP/6-311G(d,p) basis set. Therefore reduction of the $f(A)$ peak intensity for TS in comparison with that for pristine silica gels is connected to the decrease in the pore volume on the titania grafting. Textural and adsorptive properties of the initial and modified silica gels can reflect in adsorption of such polar adsorbate as water specifically interacting with different active surface sites on the oxide surfaces.

Desorption of water from unmodified and modified silica gels (Fig. 9) shows that the amounts of adsorbed water (C_{H_2O}) increase for TiO_2/KG 60 and TiO_2/KG 100 but decrease for TiO_2/KG 40 due to the impact of two opposite factors: (i) blocking and filling of pores by titania deposits, and (ii) enhancement of the hydrophilicity of mixed oxide in comparison with the initial silica (Gun'ko et al., 1998). Despite smaller V_p for KG 40 (Table 2), the concentration of adsorbed water (exposure 15 h) is greater than that for KG 60 and KG 100 (Fig. 9(a)). Water fills approximately 56% of V_p for KG 40 after exposure in the saturated water vapor for $t_w = 15$ h, but for KG 60, a similar amount of adsorbed water is observed for $t_w = 70$ h. For KG 100, C_{H_2O} ($t_w = 15$ h) corresponds to 17% of the total pore volume; i.e., the larger the pores, the smaller the portion of them is filled by water for the same time of

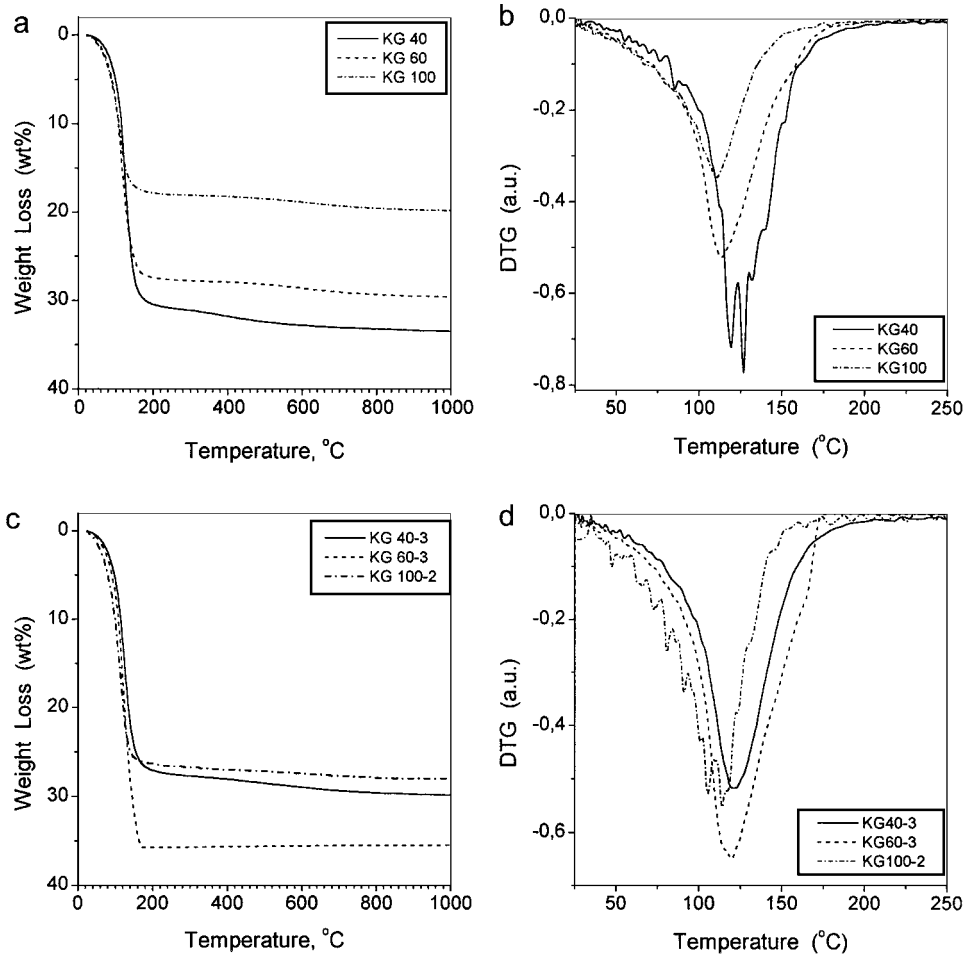

Figure 9. Desorption of water from (a, b) initial silica gels and (c, d) TS; (a, c) TG and (b, d) DTG.

exposure in the saturated water vapor. The inflection point on the DTG plots (Fig. 9) slightly shifts toward high temperature for pristine and modified KG 40 in comparison with that for adsorbents with larger pores, as the activation energy of water desorption from narrower pores can be greater. However, the difference in DTG for TiO_2/KG 40 and TiO_2/KG 60 is smaller (Fig. 9(d)) than that for the corresponding initial silica gels (Fig. 9(b)) that can be due to larger amount of titania deposits for KG 60-3 than that for KG 40-3 (Table 1), which can compensate other factors.

4. Conclusion

In the case of narrow-mesoporous KG 40, grafting of anatase crystallites occurring on the outer surfaces of silica gel causes more significant blocking of pores than that for KG 60 or KG 100 due to formation of larger TiO_2 particles with average crystallite size of 70 nm after four CVD reaction cycles on KG 40. The average size of anatase crystallites decreases with increasing average pore size: 21 nm for KG 60-4 and 16 nm for KG 100-4, which are, however, significantly larger than their average pore size; i.e., they can form on the external surfaces of silica gel grains. A greater portion of titania formed under relatively soft conditions (523 K) represents amorphous phase with its a maximal contribution after the first reaction cycle. Amorphous titania can form both in pores and on the external surfaces of silica particles. According to IR spectra, the ≡Si—O—Ti≡ bridges are absent in titania/silica due to their hydrolysis during the CVD-titania synthesis and segregation of titania into individual particles. Grafting

of titania results in changes in water adsorption, which increases for modified KG 60 and 100 but decreases for TiO_2/KG 40 due to stronger blocking of narrow pores by titania deposits.

Acknowledgments

This research was supported by NATO (Grant EST.CLG.976890), the Polish State Committee for Scientific Research and Ministry of High Education and Science of Ukraine (Grant 2M/303-99).

References

Adamson, A.W. and A.P. Gast, *Physical Chemistry of Surface*, Wiley, New York, 1997.

Avnir, D. and M. Jaroniec, "An Isotherm Equation for Adsorption on Fractal Surfaces of Heterogeneous Porous Materials," *Langmuir*, **5**, 1431–1433 (1989).

Battiston, G.A., R. Gerbasi, M. Porchia, and A. Marigo, "Influence of Substrate on Structural Properties of TiO_2 Thin Films Obtained via MOCVD," *Thin Solid Films*, **239**, 186–191 (1994).

Castillo, R., B. Koch, P. Ruiz, and B. Delmon, "Influence of Preparation Methods on the Texture and Structure of Titania Supported on Silica," *J. Mater. Chem.*, **4**, 903–906 (1994).

Crocker, M., R.H.M. Herold, A.E. Wilson, M. Mackay, C.A. Emis, and A.M. Hoogendoorn, "^{1}H NMR Spectroscopy of Titania. Chemical Shift Assignments for Hydroxy Groups in Crystalline and Amorphous Forms of TiO_2," *J. Chem. Soc., Faraday Trans*, **92**, 2791–2798 (1996).

Gregg, S.J. and K.S.W. Sing, *Adsorption, Surface Area and Porosity*, Academic Press, London, 1982.

Gun'ko, V.M., R. Leboda, W. Grzegorczyk, J. Skubiszewska-Zięba, M. Marciniak, A.A. Malygin, and A.A. Malkov, "CVD-Titania/Silica Gel Carbonized due to Pyrolysis of Cyclohexene," *Langmuir*, **16**, 3227–3243 (2000).

Gun'ko, V.M., F. Villiéras, R. Leboda, M. Marciniak, B. Charmas, and J. Skubiszewska-Zięba, "Characterization of CVD-Titania/Silica Gel by Means of Low Pressure Nitrogen Adsorption," *J. Colloid Interface Sci.*, **230**, 320–327 (2000).

Gun'ko, V.M., V.I. Zarko, E. Chibowski, V.V. Dudnik, R. Leboda, and V.A. Zaets, "Structure of Pyrogenic TiO_2 and TiO_2/SiO_2 and Influence of the Active Surface Site Nature on Interaction with Water," *J. Colloid. Interface Sci.*, **188**, 39–57 (1997).

Gun'ko, V.M., V.I. Zarko, B.A. Chuikov, V.V. Dudnik, Yu.G. Ptushinskii, E.F. Voronin, E.M. Pakhlov, and A.A. Chuiko, "Temperature-Programmed Desorption of Water from Fumed Silica, Titania, Silica/Titania, and Silica/Alumina," *Int. J. Mass Spectrom. Ion Processes*, **172**, 161–179 (1998).

Gun'ko, V.M., V.I. Zarko, V.V. Turov, R. Leboda, and E. Chibowski, "The Effect of Second Phase Distribution in Disperse X/Silica ($X = Al_2O_3$, TiO_2, and GeO_2) on its Surface Properties," *Langmuir*, **15**, 5694–5702 (1999).

Gun'ko, V.M., V.I. Zarko, V.V. Turov, R. Leboda, E. Chibowski, L. Holysz, E.M. Pakhlov, E.F. Voronin, V.V. Dudnik, and Yu.I. Gornikov, "CVD-Titania on Fumed Silica Substrate," *J. Colloid. Interface Sci.*, **198**, 141–156 (1998).

Gun'ko, V.M., V.I. Zarko, V.V. Turov, R. Leboda, E. Chibowski, E.M. Pakhlov, E.V. Goncharuk, M. Marciniak, E.F. Voronin, and A.A. Chuiko, "Characterization of Fumed Alumina/Silica/Titania in the Gas Phase and Aqueous Suspension," *J. Colloid. Interface Sci.*, **220**, 302–323 (1999).

Gun'ko, V.M. and D.D. Do, "Characterization of Pore Structure of Carbon Adsorbents Using Regularization Procedure," *Colloids Surf.* A, **193**, 71–83 (2001).

Hanprasopwattana, A., S. Srinivasan, A.G. Sault, and A.K. Datye, "Titania Coatings on Monodisperse Silica Spheres," *Langmuir*, **12**, 3173–3179 (1996).

Jaroniec, M., M. Kruk, C.P. Jaroniec, and A. Sayari, "Modification of Surface and Structural Properties of Ordered Mesoporous Silicates," *Adsorption*, **5**, 39–45 (1999).

Jaroniec, M., M. Kruk, and J.P. Olivier, "Standard Nitrogen Adsorption Data for Characterization of Nanoporous Silicas," *Langmuir*, **15**, 5410–5413 (1999).

Kiselev, A.V. and V.I. Lygin, *IR Spectra of Surface Compounds and Adsorbed Substances*, Nauka, Moscow, 1972.

Leboda, R., V.M. Gun'ko, M. Marciniak, A.A. Malygin, A.A. Malkov, W. Grzegorczyk, B.J. Trznadel, E.M. Pakhlov, and E.F. Voronin, "Structure of CVD-Titania/Silica Gel," *J. Colloid Interface Sci.*, **218**, 23–39 (1999).

Leboda, R., M. Marciniak, V.M. Gun'ko, W. Grzegorczyk, A.A. Malygin, and A.A. Malkov, "Structure of Carbonized Mesoporous Silica Gel/CVD-Titania," *Colloid. Surf.* A, **167**, 275–285 (2000).

Leboda, R., V.V. Turov, M. Marciniak, A.A. Malygin, and A.A. Malkov, "Characteristics of Hydration Layer Structure in a Porous Titania-Silica Obtained by CVD Method," *Langmuir*, **15**, 8441–8446 (1999).

Legrand, A.P. (Ed.), *The Surface Properties of Silicas*, Wiley, New York, 1998.

Nguyen, C. and D.D. Do, "A New Method for the Characterization of Porous Materials," *Langmuir*, **15**, 3608–3615 (1999).

Provencher, S.W., "A Constrained Regularization Method for Inverting Data Represented by Linear Algebraic or Integral Equations," *Comp. Phys. Comm.*, **27**, 213–227 (1982).

Szombathely, M.V., P. Brauer, and M. Jaroniec, "The Solution of Adsorption Integral Equations by Means of the Regularization Method," *J. Comput. Chem.*, **13**, 17–32 (1992).

Vansant, E.F., P. Van Der Voort, and K.C. Vrancken, *Characterization and Chemical Modification of the Silica Surface*, Elsevier, Amsterdam, 1995.